

Induced-moment spin-glass system: Nonstoichiometric PrP

S. K. Hasanain and R. P. Guertin*
Tufts University, Medford, Massachusetts 02155

K. Westerholt
Institute für Experimentalphysik, Ruhr University, Bochum, West Germany

M. Guyot[†] and S. Foner
Francis Bitter National Magnet Laboratory, Massachusetts Institute of Technology, Cambridge, Massachusetts 02139
 (Received 4 February 1981)

Stoichiometric praseodymium phosphide, PrP, has a crystalline electric field (CEF) singlet ground state and exhibits temperature-independent Van Vleck susceptibility at low temperatures. PrP does not show magnetic ordering down to 1 K. In contrast, phosphorous-deficient samples (PrP_y) show temperature-dependent susceptibilities at low temperatures, indicating an induced magnetic moment on the Pr sites. Selected samples of PrP_y for $0.95 \geq y \geq 0.85$ show spin-glass behavior. Measurements of the magnetic properties (some of which were performed in high hydrostatic pressures to 8 kbar) include: (1) high-field magnetization versus field to 60 kOe, (2) low-field magnetization versus temperature for $1.4 \leq T \leq 20$ K, and (3) ac susceptibility versus temperature over a very wide frequency range, $0.003 \leq f \leq 10^4$ Hz. The ac susceptibility measurements for PrP_{0.95} show that for $f < 1$ Hz, the spin-glass transition temperature, $T_f \approx 9$ K, is independent of f , and with hydrostatic pressure T_f increases as $dT_f/dP = +0.12$ K/kbar. Time-dependent remanent effects are observed for $T \leq T_f$. No specific-heat anomaly is discernible near T_f . Pressure-dependent magnetization measurements to 8 kbar show that the magnetic moments and/or interactions between moments increase with decreasing lattice constant, consistent with pressure studies on stoichiometric PrP. The magnetic properties of nonstoichiometric PrP_y depend strongly on lattice constant and method of preparation. Susceptibility data on PrS_{0.85} and Pr_{0.1}La_{0.9}P_{0.85}, which do not show spin-glass behavior, illustrate the influence of anion vacancies on the magnetic properties. The CEF level scheme is drastically altered by the symmetry changes produced by P vacancies, but it is believed that increased conduction-electron concentration plays an important role in inducing the Pr moments in nonstoichiometric PrP compounds.

I. INTRODUCTION

Spin-glasses are described in a general way as nonperiodic magnetic systems with random exchange fields, leading to some local magnetic order. They usually show characteristic physical properties such as: (1) a rather well-defined cusp in the temperature dependence of the low-field ac susceptibility (the temperature of this cusp often depends on the frequency of the ac magnetic field), (2) a very broad anomaly of the heat capacity in the cusp temperature range, and (3) time-dependent magnetic remanence effects. Many magnetic impurity systems are expected to exhibit some or all of the characteristics of spin-glasses over a suitable impurity concentration range. Examples of extensively studied spin-glass systems include Au(Fe),¹ Cu(Mn),² La(Gd)Al₂,³ and the insulating system Sr(Eu)S.⁴

Nonstoichiometric PrP_y is an unusual spin-glass system.^{5,6} First, only nonstoichiometric composition

compounds exhibit spin-glass behavior. In this respect, PrP_y is similar to the nonstoichiometric Co_{1+x}Ga_{1-x} spin-glass system.⁷ Secondly, the Pr ion crystalline electric field (CEF) ground state in the nonstoichiometric materials is expected to be a singlet. Thirdly, we speculate that some variation of the Pr ion moments from site to site occurs because of the variation of the Pr site local environments. In contrast, for stoichiometric PrP, the Pr ion carries no magnetic moment at low temperatures and does not order magnetically at any temperature.⁸ Furthermore, stoichiometric PrP is a singlet ground-state (Van Vleck) paramagnet with a singlet-first-excited-state splitting of 133 K.⁹ (The lower crystalline symmetry of the nonstoichiometric materials is accompanied by a further removal of degeneracy of the CEF levels.)

Singlet ground-state Pr-based compounds show a wide variety of magnetic behaviors. For Pr₃Tl the Pr moment distribution is uniform and ferromagnetic

order is observed.¹⁰ For Pr₃Se₄, ferromagnetism is also observed, but there are two types of Pr sites.¹¹ In contrast, all the stoichiometric Pr monopnictides and Pr monochalcogenides are paramagnetic and are well characterized by CEF-only behavior,⁹ i.e., the low-temperature magnetic susceptibilities are temperature independent. Thus PrP_y falls into a middle ground between these two extremes of singlet ground-state materials.

In this paper, we present the results of measurements of the magnetic properties as a function of field, temperature, and hydrostatic pressure of several PrP_y samples in the concentration range $0.97 \geq y \geq 0.85$. Magnetization studies were carried out in external fields to 60 kOe, temperatures $1.4 \leq T \leq 30$ K, and for hydrostatic pressures to 8 kbar. ac susceptibility measurements were made over a very wide frequency range of $0.003 \leq f \leq 10^4$ Hz. In addition, very-low-frequency susceptibility measurements as a function of pressure were made. In Sec. II we review the properties of some off-stoichiometric rare-earth monopnictides and monochalcogenides. Also, we calculate changes in the CEF level structure of stoichiometric PrP when P-site vacancies are introduced. In Sec. III we discuss the sample preparation required to produce spin-glass behavior in PrP_y, sample characterization, and experimental techniques. In Sec. IV we present the experimental results which include high- and low-field magnetization, ac susceptibility as a function of frequency, specific heat, time-dependent remanence effects, and pressure effects. In the final section we discuss the results of this unusual spin-glass system. Previous communications^{5,6} dealt with audio and very-low-frequency ac susceptibility characteristics of nonstoichiometric PrP_y.

II. BACKGROUND

A. Nonstoichiometric rare-earth monopnictides and monochalcogenides

The rare-earth monopnictides and monochalcogenides all have the NaCl structure, and exist over a very large range of solid solubilities. Some examples are PrP_y ($1.00 \geq y \geq 0.85$),¹² GdS_y ($1.00 \geq y \geq 0.85$),¹³⁻¹⁵ GdP_y ($1.00 \geq y \geq 0.90$),¹⁵ LaS_y ($1.00 \geq y \geq 0.90$),¹⁶ and RN_y ($y \leq 1$, R = Y, Nd, La, Ce, and Pr).¹⁷ For all these compositions the NaCl structure is preserved. The range of solubility tends to decrease with increasing ionic radius of the anion, thus compounds such as PrBi_y exist only over a very narrow range near stoichiometry. For the above systems, vacancies are formed in the anion sublattice when there are anion deficiencies. This is concluded from density measurements.¹³ The lattice parameter tends to decrease with increasing anion deficiency,

thus a measurement of the lattice-parameter decrease with increasing anion deficiency can be used to determine indirectly the concentration of vacancies. To our knowledge, a vacancy superstructure has never been observed, so it is reasonable to assume a random distribution of vacancies on the anion sublattice.

For GdP_y and GdS_y, the anion deficiency is accompanied by an increase in conduction-electron concentration.¹⁵ This is also the case for EuS.¹⁸ For the monosulfides this is supported by simple chemical reasoning: S has valence of -2 and Gd has valence of +3, thus removing an S atom should contribute two electrons to the conduction band. In the monophosphide, the situation is less clear because the bonding has more covalent character. Nevertheless, we would expect roughly three conduction electrons per vacancy from the same reasoning. Although in principle one might expect GdP to be a semiconductor, it shows metallic conduction ($dp/dT > 0$) for $4 \leq T \leq 200$ K, and as in GdS_y, an increase in conduction electron density is found for off-stoichiometric materials.¹⁵ In PrP, the compound discussed in this paper, the conduction electron density is expected to be low. (For GdP it is $\sim 1 \times 10^{21}/\text{cm}^3$ versus $2 \times 10^{22}/\text{cm}^3$ for GdS.¹⁵) Because of the semi-metallic character of the phosphide, small changes in stoichiometry might drastically increase the conduction-electron concentration and thus might have an important effect on physical properties. For example, it may cause an enhancement of the magnetic exchange interaction between Pr atoms by the Ruderman-Kittel-Kasuya-Yosida (RKKY) interaction.

B. Crystalline electric field effects in PrP_y

For all the Pr monopnictides (and monochalcogenides) the CEF of surrounding ions partially lifts the ninefold degeneracy of the Pr³⁺ spin-orbit ground state, and a nonmagnetic singlet, Γ_1 , CEF ground state results.⁹ A magnetic triplet Γ_4 is the first excited state. These compounds are nonordered magnetically and exhibit temperature-independent susceptibilities at low temperatures. This Van Vleck-like susceptibility is given, in the low-field limit, by¹⁹

$$\chi_c = \frac{2Ng_f^2 \mu_B^2 |\langle \Gamma_4 | J_z | \Gamma_1 \rangle|^2}{k_B \Delta}, \quad (1)$$

where Δ is the Γ_1 - Γ_4 splitting (in K), and where the other symbols have their usual meaning. Equation (1) gives $\chi_c = 2.40 \times 10^{-2}$ emu/mole Oe for PrP, using $\Delta = 133$ K determined by inelastic neutron scattering.⁹ The CEF parameters associated with the observed level sequence and the magnitude of Δ closely approximate those derived from a six-nearest-neighbor point-charge model (PCM) with a charge of $-2e$ on the P ions. The Lea, Leask, and Wolf

(LLW) parameters²⁰ from the neutron scattering experiments are $x = -0.944$ and $W = 7.42$ K, while those from the PCM are $x = -0.967$ and $W = 6.62$ K. The measured low-temperature susceptibility of PrP, $[(3-4) \times 10^{-2}]$ emu/mole Oe, is enhanced over the CEF-only value of Eq. (1). We speculate that this sample dependence of the susceptibility reflects small variations about the stoichiometric composition. However, the enhancement is small compared to that of the induced ferromagnet, Pr₃Tl.²¹

The observed effect of hydrostatic pressure on the magnetic properties of the Pr monopnictides (and monochalcogenides) is contrary to predictions of the PCM.^{22,23} We expect the CEF interaction to increase as neighboring ions approach the Pr ion site. Experiments show an increase in the susceptibility, χ , with decreasing lattice constant. Neutron scattering²⁴ and thermal expansion²⁵ measurements show directly that Δ decreases with increasing pressure. Phenomenological models²⁶ have been put forth to account for the anomalous pressure dependence of Δ .

Using pressure-dependent Knight-shift measurements, Weaver and Schirber²³ determined that χ for PrP increases at a rate of $(+1.6 \pm 0.2)\%/kbar$. By extension for the off-stoichiometric PrP_y materials, application of pressure should increase the Pr moments and/or the Pr-Pr magnetic coupling. This is found to be the case.

The six-nearest-neighbor PCM model explains semiquantitatively the magnetic behavior of stoichiometric PrP. For PrP, which has the cubic rocksalt structure, the CEF Hamiltonian is²⁷

$$H_{\text{CEF}}^{\text{C}} = B_{40}O_4^0 + B_{44}O_6^0 + B_{60}O_6^0 + B_{64}O_6^4, \quad (2)$$

where $B_{nm} = b_{nm}Qe^2/a^{n+1}\langle r^n \rangle \alpha_n$. The b_{nm} values are $b_{40} = \frac{7}{16}$, $b_{44} = \frac{35}{16}$, $b_{60} = +\frac{3}{64}$, and $b_{64} = -\frac{63}{64}$. The symbols O_n^m are Stevens operator equivalents. The PCM values of x and W are obtained by diagonalizing Eq. (2).

In order to illustrate the rather drastic effect of P-site vacancies we calculate the CEF level structure for the case of two nearest-neighbor collinear P-site vacancies, ignoring any changes of screening or local distortions. The results are shown in Fig. 1. The Hamiltonian for this symmetry is similar to that of Eq. (2) but also contains a term $B_{20} = Qe^2\langle r^2 \rangle/a^3$. The terms b_{40} and b_{60} become $\frac{3}{16}$ and $-\frac{5}{64}$, respectively, but the b_{44} terms and b_{64} terms are unchanged from the cubic case. The sixth-order terms were set to zero, which closely approximates the real case for cubic PrP. The diagonalized eigenvalues are parametrized by $z = B_{20}/B_{40}^{\text{C}}$, the superscript C referring to the cubic value for this term. Even for $z=0$ the eigenvalues shift because of the new relative weight of B_{40} and B_{44} . The scale of the vertical axis in Fig. 1 is such that $\Delta = 133$ K. The value of z derived from the B_{nm} above is off the scale of Fig. 1.

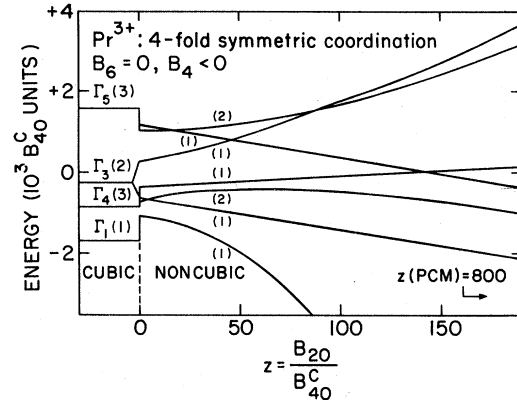


FIG. 1. Crystalline electric field (CEF) energy levels for Pr³⁺ in PrP_y for the case of two collinear nearest-neighbor vacancies. The horizontal scale is proportional to the magnitude of the second-order CEF Hamiltonian term. Vertical scale in units of CEF fourth-order cubic Hamiltonian terms. The Γ_1 - Γ_4 splitting is 133 K for cubic PrP. Sixth-order terms are neglected. Numbers in parentheses indicate level degeneracy. Point-charge-model value for z is off the scale of the figure. The figure illustrates drastic effect on CEF level structure upon introduction of vacancies into anion sublattice.

Clearly from Fig. 1, in spite of level crossings, the nonmagnetic ground state is retained. An analysis like the above for a *single* nearest neighbor vacancy resulted in a diagram similar to that in Fig. 1.

These calculations are not expected to yield the actual CEF level scheme for Pr in nonstoichiometric PrP_y materials. Because of the importance of the B_{20} term (r^{-3} dependence) relative to the other CEF Hamiltonian terms, vacancies many lattices away from a given Pr site would have a strong effect on the CEF level scheme if shielding effects are unimportant. Nevertheless, the results shown in Fig. 1 point out the strong influence on the CEF levels by changes in local symmetry. Furthermore, they suggest that in general a singlet ground state is maintained for Pr in nonstoichiometric PrP and that the moments observed under these circumstances are "induced." A discussion of induced magnetism in singlet ground-state systems is given by Cooper for both ferro-¹⁹ and antiferromagnetic²⁸ materials. Within the molecular-field approximation, the presence of a molecular field mixes excited states with the singlet ground state so that the expectation value of the magnetic moment for the perturbed ground state becomes nonzero, and magnetic order can occur. Examples of such systems are Pr₃Tl (Ref. 10) (an induced ferromagnet) and TbSb (Ref. 28) (an induced antiferromagnet), where in both cases inelastic neutron scattering shows a perturbed singletlike ground state. We believe that moments are induced on Pr sites in PrP_y in a similar manner.

The experimental data in Fig. 2 show the influence of vacancies on the magnetic properties of two singlet ground-state Pr-based monpnictides and monochalcogenides. The upper part of the figure shows χ^{-1} vs T for PrS and PrS_{0.85}. For PrS, $\Delta = 125$ K,⁹ and the data show the characteristic temperature independent susceptibility for $T \leq 50$ K. However, for nonstoichiometric PrS_{0.85} the temperature-independent part has vanished, and χ^{-1} vs T is linear down to lowest T . In the lower part of the figure similar data are seen for PrP and Pr_{0.1}La_{0.9}P_{0.85}. (The La-diluted sample is chosen because PrP_{0.85} orders magnetically and cannot be compared directly to the PrS_{0.85} data.) We note in Fig. 2 that the $\chi^{-1} = 0$ intercept for the nonstoichiometric materials occurs at $T < 0$. These materials are nonordered and have large strong crystal-field contributions to χ . For the PrP_y samples which undergo spin-glass ordering, the $\chi^{-1} = 0$ intercept is at $T > 0$, indicating a tendency for ferromagnetic coupling. In stoichiometric PrP (Ref. 5) a ferromagnetic exchange is postulated to explain the low-temperature susceptibility which is slightly enhanced over the crystal-field-only value. The data of Fig. 2 demonstrate the presence of a magnetic moment on Pr sites in nonstoichiometric samples. In contrast, for stoichiometric cases, the expectation value of the magnetic moment is zero for the CEF ground state. Data on GdS and GdP (Ref. 15) show that the presence of S- or P-site vacancies is accompanied by an increase in conduction-electron concentration. We expect this also to be the case for the nonstoichiometric materials of Fig. 2.

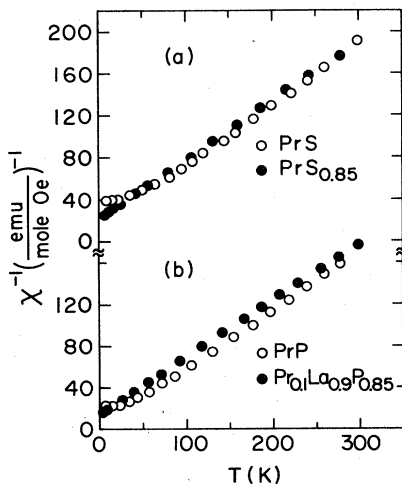


FIG. 2. Inverse magnetic susceptibility, χ^{-1} , vs temperature, T , for two singlet ground-state materials, PrS and PrP, and two nonstoichiometric counterparts. In both cases, χ becomes temperature dependent for $T \leq 30$ K when vacancies are introduced into the anion sublattice.

III. EXPERIMENTAL RESULTS

A. Sample preparation

The method of sample preparation plays a very important role in determining whether spin-glass behavior in PrP_y is observed. Nearly two dozen samples were prepared. The general procedure for sample preparation was as follows^{12,5}: Thin foils (≤ 0.01 cm), or in some cases thin slivers, of high-purity ($\geq 99.9\%$) Pr were reacted with 99.999% pure P powder in sealed quartz tubes for a few days at 600 °C until P vapor no longer remained in the tube. The powdery reacted material was then compacted into pellets, sealed into Ta foil or Mo crucibles, and heat treated for an homogenization at 1800 °C for 4 h. Only those materials which had been compacted showed the spin-glass behavior. In some cases, off-stoichiometric, noncompact samples tended to show a temperature-dependent χ similar to data in Fig. 2. Compacted samples were rather hard, had a metallic luster, and were porous.

The lattice constants for all off-stoichiometric compounds⁵ that showed spin-glass behavior were found to be smaller than those for pure PrP, by about 0.5%. Off-stoichiometric samples that showed no cusp in $\chi(T)$ were found to have lattice constants close to those of pure PrP. A second phase (PrP₂) was detected in only one sample.

B. Experimental procedures

The dc magnetization experiments were performed using a vibrating sample magnetometer (VSM). The ac susceptibility measurements were made with a conventional ac susceptibility bridge for $10 \leq f \leq 10^4$ Hz. The ac measurements in the range $0.003 \leq f \leq 0.03$ Hz involved a novel application of the VSM.⁶ This method allowed determination of the in-phase component χ' of the susceptibility, and also of the out-of-phase component χ'' . For those experiments requiring the application of hydrostatic pressure, non-magnetic pressure clamp devices were attached to the VSM. These techniques are described in Ref. 29. The very low frequency susceptibility measurements with the sample pressurized illustrate the versatility of the pressure clamp procedures used normally in connection with high dc field studies.

C. dc magnetic properties

As noted first by Westerholt and Methfessel,⁵ low-temperature, low-field dc susceptibility anomalies are observed in selected off-stoichiometric PrP_y samples. Although this is easily seen with dc techniques, the position of the observed peak in χ depends on the

strength of the measuring field and time rate of change of the temperature. This latter effect is not due to a lack of thermodynamic equilibrium between thermometer and sample, but involves time-dependent magnetization effects which were discovered in PrP_y for low (≤ 1 kOe) applied fields. These effects occur for all temperatures below that at which the gradual spin freezing process takes place, and they will be discussed below. A related effect is the shift with frequency of the susceptibility peak in PrP_y using ac measurements.

In Fig. 3 is shown the magnetic moment σ , versus applied field, H_0 for three PrP_y samples at 4.2 K in fields to 50 kOe. The saturated Pr^{3+} moment is $3.2 \mu_B/\text{Pr-atom}$, so that σ at high fields in off-stoichiometric materials is substantial. The large moment per Pr atom and the nonlinearity of σ vs H_0 suggest a moment on the Pr ion. For $\text{PrP}_{1.00}$, also shown in Fig. 3, σ vs H_0 is linear. The dashed line associated with $\text{PrP}_{1.00}$ shows the increase of χ expected for a pressure 10 kbar based on the data of Ref. 23. The induced Pr moments (those responsible for a T -dependent χ for $T \leq 30$ K) are also responsible for the spin-glass freezing and for the curvature of the magnetization versus H_0 of Fig. 3. We note that for $H_0 \geq 1$ kOe, time-dependent effects are not observed; the moment responds rapidly to changes in applied field.

The insert of Fig. 3 shows the low field χ vs T data for the $\text{PrP}_{0.95}$ and $\text{PrP}_{0.85}$ samples. We note that the positions of the maxima depend to some extent on the rate of change of the temperature, because of the time-dependent effects mentioned above. We define a "freezing" temperature T_f as the maximum in χ vs T for our PrP_y samples showing spin-glass behavior.

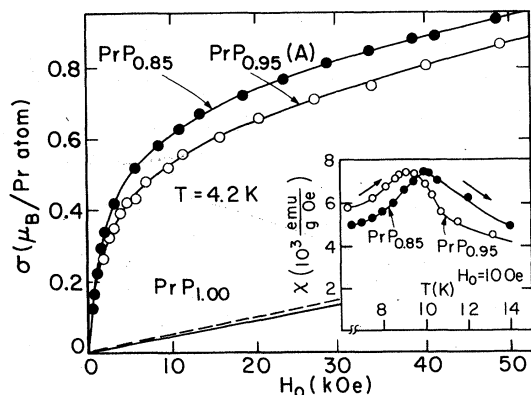


FIG. 3. Magnetization, σ , vs applied field, H_0 , at 4.2 K for two nonstoichiometric PrP_y samples, as well as data for stoichiometric $\text{PrP}_{1.00}$. Insert is low-field χ vs T for same two samples, showing spin-glass transition region. Dashed line shows σ vs H_0 at 10 kbar for $\text{PrP}_{1.00}$, based on data of Ref. 23. Saturation moment for Pr^{3+} is $3.2 \mu_B/\text{Pr atom}$.

Measurements also were made on a $\text{Pr}_{0.5}\text{La}_{0.5}\text{P}_{0.85}$ sample where half the Pr atoms are replaced by non-magnetic La atoms. This material showed pronounced time-dependent effects for $T \leq 3$ K.

In Fig. 4, are shown σ vs T data for a $\text{PrP}_{0.90}$ sample taken with three different applied magnetic fields. As the field is increased a broadening of the maxima and lowering of T_f occurs. These data emphasize the variability (and difficulty) in the characterization of the spin-glass region by dc techniques.

The results of χ vs T for two additional PrP_y samples is shown in Fig. 5. These samples were prepared as were those samples discussed above but were not compacted prior to homogenization. Whereas χ for $\text{PrP}_{0.95}$ has a clear temperature dependence, showing a moment on Pr sites, χ for $\text{PrP}_{0.97}$ is temperature independent up to ~ 16 K but is strongly enhanced over χ for the stoichiometric material. No spin-glass transition was observed in either sample, but the results illustrate the increase in Pr magnetic moment that occurs with increasing P deficiency.

In Fig. 6, we show the results of thermoremanent magnetization (TRM) measurements in the same $\text{PrP}_{0.95}$ sample discussed in Fig. 3, i.e., where the maximum in χ occurs at about 9 K. For the data of Fig. 6, the sample was cooled from above ~ 20 K to the indicated temperature in an external field of 20 Oe, which was then switched off at time $t = 0$. Between each run the sample was warmed to well above 20 K in order to remove any magnetic "history," before the 20-Oe field was applied. In all cases, after the field was switched off, the magnetization, σ , dropped very rapidly at first, then proceeded to decay slowly. The value of the remanent moment just after switching off the field increased very strongly with decreasing temperature, similar to that

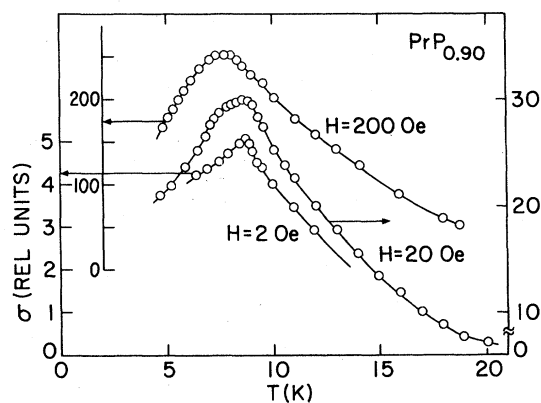


FIG. 4. Magnetization vs increasing temperature for $\text{PrP}_{0.90}$ sample taken with three widely differing measuring fields. Note temperature decrease and broadening of spin-glass transition region with increasing measuring field.

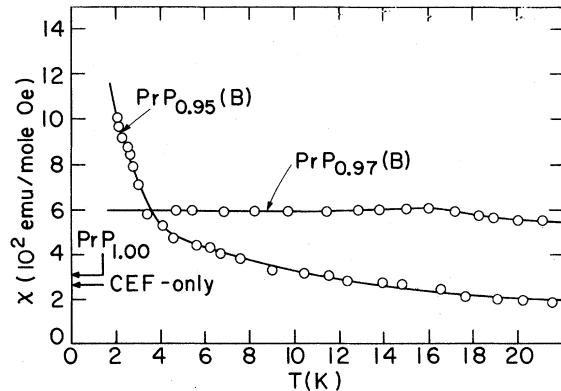


FIG. 5. Susceptibility vs temperature for two PrP_y samples which show no spin-glass transition. Susceptibility for $\text{PrP}_{0.97}$ is highly enhanced over CEF-only value, and $\text{PrP}_{0.95}$ shows indication of magnetic moment on pr ions.

observed in $\text{Au}(\text{Fe})$.¹ The agreement between this slow decay and $\log t$ is quite satisfactory. TRM decay is discussed in detail by Guy in extensive review articles,¹ and the data of Fig. 6 show a close resemblance to those analogous data for $\text{Au}(\text{Fe})$. The logarithmic behavior of σ vs t in Fig. 6 is characteristic of spin-glass systems; the results follow in form those simulated by the computer model by Binder and Schröder,³⁰ who find a $t^{-\alpha}$ decay using Edwards and Anderson's³¹ model of a random distribution of exchange constants.

The low-field time-dependent (TRM) effects can be used to indicate roughly the onset of the spin-glass freezing process. As noted by Guy¹ and Binder and Schröder,³⁰ the slow decay behavior persists to tem-

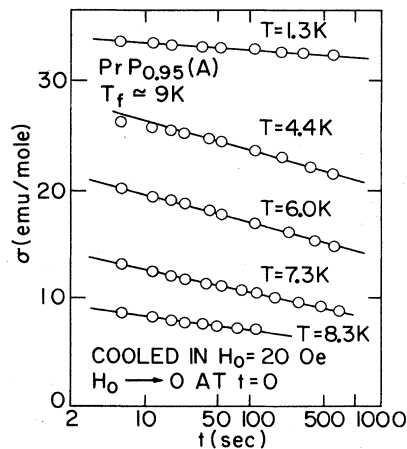


FIG. 6. Thermoremanent magnetization (TRM) vs time for $\text{PrP}_{0.95}$ sample. Sample was warmed before each measurement to $T \approx 20$ K before cooling in 20-Oe field.

peratures above the χ vs T peak. This is illustrated for the $\text{PrP}_{0.95}$ sample in Fig. 7, where $\sigma(t=1000 \text{ sec})$ vs T is shown. Taking the values of σ at $t=1000 \text{ sec}$ is merely representative of the time scale over which the logarithmic decay takes place. Choosing any t in the range 10–1000 sec does not substantially alter the results. These data were taken from those of Fig. 6. Clearly the slow decay mechanisms persist at temperatures above the χ vs T maximum. The uppermost curve in Fig. 7 shows χ vs T on cooling in the 20-Oe field. Note that the temperature at which the two upper curves depart (about 10 K) is above the maximum in χ vs T and is close to that where the time independence of σ vanishes. For this sample, the higher temperature is taken as the onset of the gradual spin-glass freezing process.

The specific heat C vs T for a $\text{PrP}_{0.85}$ sample which shows spin-glass behavior below about 10 K is shown in Fig. 8. Specific-heat data on LaP_y , an isomorphic, nonmagnetic analog for PrP_y , are not available, so it is difficult to determine the magnetic part of the specific heat. The results for PrP_y are, however, similar to those for $\text{Au}_{0.92}\text{Fe}_{0.08}$,³² where the magnetic part of the specific heat is linear with temperature, but where no specific-heat anomaly accompanies T_f , the freezing temperature. Specific-heat anomalies for spin-glass systems are generally quite small, possibly reflecting a gradual freezing process. In addition, for PrP_y , which is a singlet ground-state system, there is probably only a small amount of CEF entropy remaining near 10 K. It is interesting to compare the results of Fig. 8 with that of Pr_3Tl , also a singlet ground-state material, and also with only a small

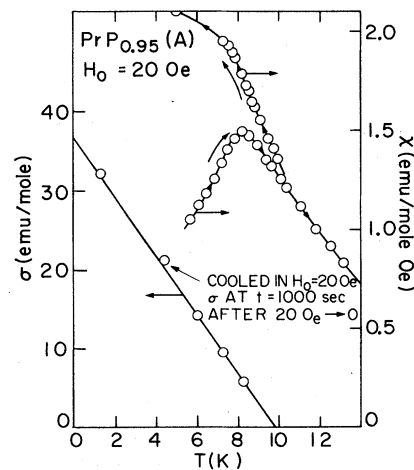


FIG. 7. Lower part of figure: TRM vs temperature, T , evaluated at $t=1000 \text{ sec}$, showing persistence of time-dependent effects above $T_f=9 \text{ K}$, where susceptibility is maximum. Upper part of figure: χ measured in 20 Oe field as T is lowered, and χ as measured in 20 Oe as T is raised after cooling in zero field.

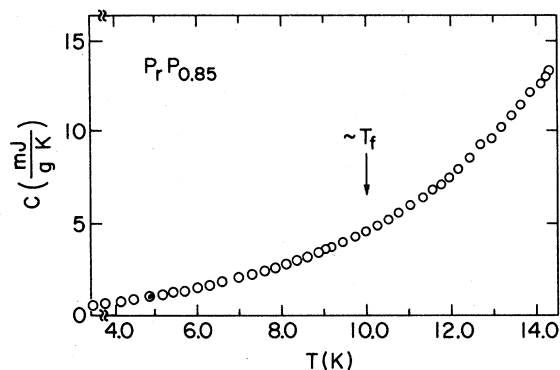


FIG. 8. Specific heat vs temperature for $\text{PrP}_{0.85}$, showing no anomaly in range of spin-glass transition temperature.

amount of CEF entropy remaining at its ferromagnetic ordering temperature, 12 K. In this latter case an anomaly in C vs T of ~ 5 mJ/g K is observed.³³

D. ac magnetic properties

The characteristic maximum in the ac susceptibility of PrP_y is quite narrow. We have investigated its frequency dependence over a very wide range, $0.003 \leq f \leq 10^4$ Hz. Two different methods were used; the details of the techniques may be found in Ref. 6. A conventional ac susceptibility bridge was used for $f > 10$ Hz, and a VSM was employed in a novel manner for measurements for $f \leq 0.03$ Hz. The results of these measurements are shown in Fig. 9 for two $\text{PrP}_{0.85}$ samples. For $f \geq 1$ Hz a clear frequency dependence is observed, and T_f^{-1} varies as $\log f$, in agreement with other systems.³⁴ Here, T_f is defined as the maximum in χ_{ac} . The difference in

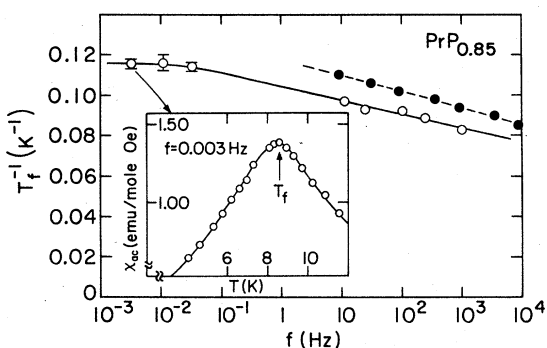


FIG. 9. Temperatures, T_f , of ac susceptibility maxima vs measuring frequency over wide frequency range. Solid circles denote different sample with same nominal concentration. Data show frequency independence of T_f for $f \leq 1$ Hz. Insert shows example of very-low-frequency susceptibility data. Similar results found for $\text{PrP}_{0.95}$ sample.

the data between the two samples (circles and solid circles) illustrates the variability in T_f for our different samples having the same nominal concentration of P vacancies.

For $f \leq 1$ Hz, T_f becomes frequency independent.³⁵ We attribute the frequency independence of T_f to the fact that the relaxation frequencies of the magnetization are large compared to the measuring frequency. In addition to the results shown in Fig. 9, we note that the technique also allows the determination of a quantity proportional to the out-of-phase component χ'' of the susceptibility (the "loss" component). As noted in Ref. 6, χ'' for $\text{PrP}_{0.85}$ increases to a maximum about 2 K below T_f , but is nonzero for about 2 K above T_f . The ratio χ''/χ' changes only over the region $6 \leq T \leq 11$ K, below which it is constant. We believe the data indicate a continuous freezing process taking place over this temperature range. For $T < 6$ K in this sample, χ'' is proportional to χ' . For $T > 11$ K, the system is entirely paramagnetic and there is rapid response of the uncoupled moments to the slowly varying fields, and any small out-of-phase response to the field observed is due to time constants associated with the VSM amplifier. In the insert of Fig. 9, we see χ' vs T for the $f = 0.003$ Hz data. It was found that for low-frequency ac fields of less than about 20 Oe, there was no change in the temperature dependence of χ' or χ'' .

Concluding this section, we emphasize that PrP_y shows a response to alternating fields that is typical of spin-glasses, at least for $f \geq 1$ Hz. A saturation (a constant minimum in T_f) is noted for $f \leq 1$ Hz. Using the low-frequency method of measurement an identification is made of the freezing temperature range for this spin-glass system. This technique should be applicable for tests of the low-frequency dynamics of other, more conventional, spin-glass systems.

E. Effects of hydrostatic pressure

As mentioned in Sec. II above, hydrostatic pressure increased the magnitude of the Pr moment and/or the Pr-Pr interaction strength. This is analogous to the result found in stoichiometric PrP, where there is a 1.6%/kbar increase in the low-temperature magnetic susceptibility.²³ In Fig. 3, the dashed line associated with the $\text{PrP}_{1.00}$ data shows this effect for a pressure of 10 kbar.

Two experiments were carried out to determine the effect of pressure on PrP_y samples. The first was a measurement of the magnetization versus applied field (σ vs H_0) to 50 kOe at 4.2 K in $\text{PrP}_{0.95}$ subjected to high pressures. The results of several such measurements show an increase in the high-field moment of about 0.4%/kbar. No substantial change was

noted in the shape of the σ vs H_0 curve. The increase in σ is consistent with analogous $\text{PrP}_{1.00}$ data, where pressure caused a reduction of the CEF interaction strength (reduction in Δ for the cubic case).

The second series of experiments performed were low-frequency ($f=0.03$ Hz) ac susceptibility measurements, using the VSM and pressure clamp devices. The data in Fig. 10 show an increase of T_f of $+0.12$ K/kbar. This is a larger increase in T_f with pressure than observed for the Ag(Mn) system by Hardebusch *et al.*,³⁶ where it was concluded that the RKKY indirect Mn-Mn coupling increase accounted for the results. The pressure dependence of T_f (see Fig. 10) may be caused by: (1) the reduction in the CEF interaction strength observed in $\text{PrP}_{1.00}$ and discussed in connection with the high-field data; (2) a Pr-Pr interaction enhancement via direct or RKKY coupling, due merely to closer proximity of the ions; and/or (3) the pressure-induced increase in the electron concentration, which could result in increased shielding of the crystalline electric fields, or modification of the RKKY coupling. In analogy with the case of GdP_y ,¹⁵ we expect the electron concentration in PrP_y to be strongly dependent on lattice constant. Therefore, pressure-induced changes in electron conduction may be very large and the third mechanism may be dominant.

IV. CONCLUSIONS

Previously studied spin-glass systems generally have been formed by introducing small amounts of magnetic impurities into nonmagnetic hosts. This may lead to clusters of moments so that their distribution is no longer random throughout the matrix. However, most theoretical models assume a statistical distribution of moments. The system PrP_y should be rather well behaved with respect to moment clustering (although vacancy clustering cannot be ruled out). Unlike other systems, the moments in PrP_y are produced indirectly: disturbances are introduced in the CEF level structure, and due to the lowered symmetry at some sites on the Pr sublattice, the singlet ground state is preserved. On some sites a stable

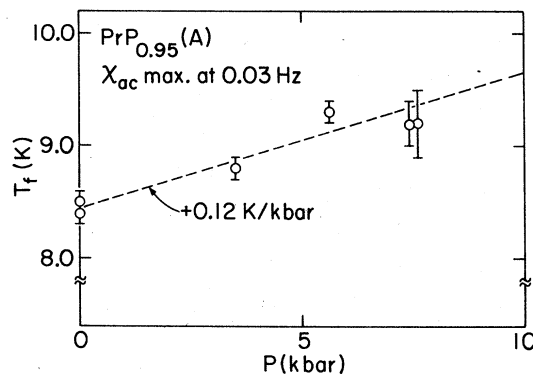


FIG. 10. Temperature of $f=0.03$ Hz susceptibility maximum vs hydrostatic pressure for $\text{PrP}_{0.95}$ sample. $P=0$ data were rerun after high-pressure data.

magnetic moment can be induced. A new feature of this system is that due to the variation from site to site of local environmental effects, e.g., CEF splitting a spatial variation of the magnitude of the Pr ground-state moments should occur. Unlike more conventional spin-glass systems, the local moment in singlet ground-state systems depends on the ratio of exchange to CEF splitting.¹⁹ It is the interactions between Pr moments that give rise to the observed spin-glass behavior. For PrP_y , these moments are distributed spatially in a random way and may have some variation in their magnitude. Despite the dissimilar origin of local moments in PrP_y compared with conventional spin-glasses, the macroscopic features of this and more conventional spin-glasses seem to be similar.

ACKNOWLEDGMENTS

We would like to thank Professor John Huber for providing expert guidance in the preparation of samples. One of us (R.P.G) was supported by NSF Grant No. DMR80-10530. The Francis Bitter National Magnet Laboratory is supported by the National Science Foundation.

*Visiting scientist appointment at the Francis Bitter National Magnet Laboratory, M.I.T., Cambridge, Mass. 02139.

†Permanent address: CNRS, Bellevue, 92190 Meudon, France.

¹C. N. Guy, *J. Phys. F* **7**, 1505 (1977); **8**, 1309 (1978).

²R. W. Kaitler, J. S. Kouvel, and H. Claus, *J. Magn. Magn. Mater.* **5**, 356 (1977); E. M. Gray, *J. Phys. F* **9**, L167 (1979).

³H. V. Lohneysen, J. L. Tholence, and R. Tournier, *J. Phys. (Paris)* **39**, C6-922 (1978); H. V. Lohneysen and J. L. Tholence, *J. Magn. Magn. Mater.* **15-18**, 171 (1980).

⁴F. Holtzberg, J. L. Tholence, H. Godfrin, and R. Tournier, *J. Appl. Phys.* **50**, 1717 (1979); K. Westerholt, U. Scheer, and S. Methfessel, *J. Magn. Magn. Mater.* **15-18**, 823 (1980).

⁵K. Westerholt and S. Methfessel, *Physica (Utrecht)*

- 86–88B, 1160 (1977).
- ⁶M. Guyot, S. Foner, S. K. Hasanain, R. P. Guertin, and K. Westerholt, *Phys. Lett. A* **79**, 339 (1980).
- ⁷M. W. Meisel, W. P. Halperin, Y. Ochiai, and J. O. Brittain, *J. Phys. F* **10**, L105 (1980); R. Cywinski and E. M. Gray, *Phys. Lett. A* **77**, 284 (1980).
- ⁸T. Tushida and W. E. Wallace, *J. Chem. Phys.* **43**, 2885 (1965).
- ⁹R. J. Birgeneau, E. Bucher, J. P. Maita, L. Passell, and K. C. Turberfield, *Phys. Rev. B* **8**, 5345 (1973).
- ¹⁰K. Andres, E. Bucher, S. Darack, and J. P. Maita, *Phys. Rev. B* **6**, 2716 (1972); see also R. P. Guertin, J. E. Crow, F. P. Missell, and S. Foner, *ibid.* **17**, 2183 (1978), for pressure effects.
- ¹¹E. Bucher, K. Andres, F. J. DiSalvo, J. P. Maita, A. C. Gossard, A. S. Cooper, and G. W. Hull, Jr., *Phys. Rev. B* **11**, 500 (1975). For pressure effects see R. P. Guertin, S. Foner, B. R. Cooper, and R. Siemann, *J. Magn. Magn. Mater.* **15–18**, 11 (1980).
- ¹²E. Franceschi and J. L. Olcese, *J. Phys. Chem. Solids* **30**, 903 (1969).
- ¹³G. Buzzone and G. L. Olcese, in *Propriétés Thermodynamique, Physiques et Structurales des Dérivés Semi-Metalliques* (CNRS, Paris, 1965), p. 387.
- ¹⁴W. Beckenbaugh, J. Evers, G. Guntherodt, E. Kaldis, and P. Wachter, *J. Phys. Chem. Solids* **36**, 239 (1975).
- ¹⁵P. Wachter, E. Kaldis, and R. Hauger, *Phys. Rev. Lett.* **40**, 1404 (1978); P. Wachter, *Phys. Rep.* **44**, 159 (1978).
- ¹⁶R. Hauger, E. Kaldis, G. van Schulthess, P. Wachter, and C. Zurcher, *J. Magn. Magn. Mater.* **3**, 103 (1976).
- ¹⁷H. Holleck, E. Smailos, and F. Thummler, *J. Nucl. Mater.* **32**, 281 (1969).
- ¹⁸Y. Shapira and T. B. Reed, *Phys. Rev. B* **5**, 4877 (1972).
- ¹⁹B. R. Cooper, *Phys. Rev. B* **6**, 2730 (1972).
- ²⁰K. R. Lea, M. J. M. Leask, and W. P. Wolf, *J. Phys. Chem. Solids* **23**, 1381 (1962).
- ²¹R. J. Birgeneau, J. Als-Nielsen, and E. Bucher, *Phys. Rev. B* **6**, 2724 (1972).
- ²²R. P. Guertin, J. E. Crow, L. Longinotti, E. Bucher, L. Kupferberg, and S. Foner, *Phys. Rev. B* **12**, 1005 (1975).
- ²³H. T. Weaver and J. E. Schirber, *Phys. Rev. B* **14**, 951 (1976).
- ²⁴C. Vettier, D. B. McWhan, E. I. Blount, and G. Shirane, *Phys. Rev. Lett.* **39**, 1028 (1977).
- ²⁵H. R. Ott and B. Luthi, *Phys. Rev. Lett.* **36**, 600 (1976).
- ²⁶R. A. B. Devine, in *Crystalline Electric Field and Structural Effects in f-Electron Systems*, edited by J. Crow, R. P. Guertin, and T. W. Mihalasin (Plenum, New York, 1980), pp. 165–71.
- ²⁷M. T. Hutchings, in *Solid State Physics*, edited by F. Seitz and D. Turnbull (Academic, New York, 1964), pp. 227–73.
- ²⁸B. R. Cooper and O. Vogt, *Phys. Rev. B* **1**, 1218 (1970).
- ²⁹R. P. Guertin, in *High Pressure and Low Temperature Physics*, edited by C. W. Chu and J. A. Woollam (Plenum, New York, 1977) pp. 97–114.
- ³⁰K. Binder and K. Schröder, *Solid State Commun.* **18**, 1361 (1976).
- ³¹S. F. Edwards and P. W. Anderson, *J. Phys. F* **5**, 965 (1975).
- ³²L. E. Wenger and P. H. Keesom, *Phys. Rev. B* **11**, 3497 (1975).
- ³³P. Bossard, S. Bakanowski, J. E. Crow, and T. Mihalasin, *J. Appl. Phys.* **50**, 1892 (1979).
- ³⁴See, for example, Ref. 3 or G. Zibold, *J. Phys. F* **8**, L229 (1978).
- ³⁵In addition to the data of Ref. 6, we note more recent results reporting the frequency independence of T_f at low frequencies. [N. Bontemps, J. C. Rivoal, M. Billardon, J. Rajchenbach, and J. Ferré, *J. Appl. Phys.* **52** (3), 1760 (1981)]. See also, E. D. Dahlberg, M. Hardiman, R. Orbach, and J. Souletie, *Phys. Rev. Lett.* **42**, 401 (1979). In this paper T_f is found to be frequency independent ($16 \leq f \leq 2.8 \times 10^6$ Hz) for very low concentration Ag(Mn) alloys. The point made is that the frequency dependence of T_f is observed in more concentrated systems, in accordance with the Néel clustering model. Although we have no measure of the moment concentration in PrP_y, our results would indicate that the samples investigated fall into the more concentrated regime.
- ³⁶U. Hardebusch, W. Gerhardt, and J. S. Schilling, *Phys. Rev. Lett.* **44**, 352 (1980).